© 2018. Published by The Company of Biologists Ltd | Journal of Experimental Biology (2018) 221, jeb176099. doi:10.1242/jeb.176099

RESEARCH ARTICLE

Smashing mantis shrimp strategically impact shells

R. L. Crane[1,*,§], S. M. Cox[2,‡], S. A. Kisare[1] and S. N. Patek[1]

ABSTRACT

Many predators fracture strong mollusk shells, requiring specialized weaponry and behaviors. The current shell fracture paradigm is based on jaw- and claw-based predators that slowly apply forces (high impulse, low peak force). However, predators also strike shells with transient intense impacts (low impulse, high peak force). Toward the goal of incorporating impact fracture strategies into the prevailing paradigm, we measured how mantis shrimp (*Neogonodactylus bredini*) impact snail shells, tested whether they strike shells in different locations depending on prey shape (*Nerita* spp., *Cenchritis muricatus*, *Cerithium* spp.) and deployed a physical model (Ninjabot) to test the effectiveness of strike locations. We found that, contrary to their formidable reputation, mantis shrimp struck shells tens to hundreds of times while targeting distinct shell locations. They consistently struck the aperture of globular shells and changed from the aperture to the apex of high-spired shells. Ninjabot tests revealed that mantis shrimp avoid strike locations that cause little damage and that reaching the threshold for eating soft tissue is increasingly difficult as fracture progresses. Their ballistic strategy requires feed-forward control, relying on extensive pre-strike set-up, unlike jaw- and claw-based strategies that can use real-time neural feedback when crushing. However, alongside this pre-processing cost to impact fracture comes the ability to circumvent gape limits and thus process larger prey. In sum, mantis shrimp target specific shell regions, alter their strategy depending on shell shape, and present a model system for studying the physics and materials of impact fracture in the context of the rich evolutionary history of predator–prey interactions.

KEY WORDS: Shell fracture, Durophagy, Stomatopod, Physical model, Behavioral plasticity, Mollusk

INTRODUCTION

The co-evolution of hard-shelled mollusks and their predators presents a model for evolutionary escalation between predators and prey (Vermeij, 1977, 1987). Shells are highly effective defensive structures that must withstand a variety of attacks, including drilling, shell breakage and being swallowed whole, as their predators, in turn, often wield specialized weapons (Chai et al., 2009; Constantino et al., 2011; Lucas et al., 2008; Vermeij, 1987; West et al., 1991; Zipser and Vermeij, 1978). Fracture of mollusk shells, a common method of durophagy, has been studied primarily in terms of the slow crushing forces of jaws and claws and through the use of materials-testing machines (e.g. Blundon and Vermeij, 1983; Buschbaum et al., 2007; Fisher, 2010; Kolmann et al., 2015; Preston et al., 1996; Vermeij and Currey, 1980). Studies of predator strategy when fracturing mollusk shells have illuminated how morphological as well as behavioral plasticity can be important to a predator's successful use of a weapon (Baldridge and Smith, 2008; Buschbaum et al., 2007; Schaefer and Zimmer, 2013; Zipser and Vermeij, 1978). However, the mechanics underlying morphological and behavioral plasticity are difficult to represent using the standard mechanical tests of shell strength. Furthermore, predatory attacks that rely on fracture through impact failure remain infrequently studied. Here, we integrated behavior, biomechanics and physical modeling to create a foundational understanding of predation using an impact weapon.

Predators often rely on multiple behavioral strategies against the defenses of hard-shelled mollusks. With specialized claws, crabs crush shells, peel back shell lips and pull snails from undamaged shells (Edgell and Rochette, 2009), often targeting particular shell regions (Boulding and LaBarbera, 1986; Elner, 1978; Zipser and Vermeij, 1978). Many crabs increase their pace or efficiency in opening shells through behavioral plasticity as well as morphological plasticity of their crushing claws (e.g. *Carcinus maenas*: Baldridge and Smith, 2008; Edgell and Rochette, 2009; *Cancer productus*: Smith and Palmer, 1994). The exceptional invasive success of the European green crab, *Carcinus maenas*, is in part attributed to its ability to adjust its behavioral strategies across prey types (Schaefer and Zimmer, 2013). Shell fracture and morphology are currently understood largely in terms of long-duration crushing predators like crabs that use high-impulse (N s; integral of force with respect to time), low-force (N) strategies; however, other predators impact shells using high peak force and low-impulse strikes, including birds, mantis shrimp and otters. Oystercatchers (*Haematopus ostralegus*) vary their impact behaviors (Le Rossignol et al., 2011; Nagarajan et al., 2002, 2015), yet few other studies have examined impact-based predatory behaviors, and the biological significance of any differences in fracture mechanics underlying these systems remains unclear.

The integration of biomechanics with behavioral strategies is central to understanding the evolution of shell morphology and the role of shell fracture. Shell strength is typically tested by slowly compressing a shell between two parallel plates until failure (method described in Vermeij and Currey, 1980; e.g. Bourdeau, 2010; Edgell and Rochette, 2008; Fisher, 2010; Preston et al., 1996). Strength tests of this kind, however, do not always capture key aspects of predation. Most predator weapons are more morphologically variable than two flat plates (Chai et al., 2009; Constantino et al., 2011; Crofts and Summers, 2014; Kolmann et al., 2015) and apply dynamic or repeated loads (Boulding and LaBarbera, 1986). Predators often attack certain regions of the shell or apply other behaviors such as peeling or impacting, which are not captured in the typical two-plate test. Using multiple methods to quantify strength of the limpet *Patella vulgata*, Taylor (2016) demonstrated differences between the impact strength, quantified by dropping rods onto shells, and the strength as measured with a more traditional two-plate crushing test.

[1]Biology Department, Duke University, Durham, NC 27708-0338, USA. [2]Organismic and Evolutionary Biology Graduate Program, University of Massachusetts Amherst, Amherst, MA 01003-9316, USA.
*Present Address: Hopkins Marine Station of Stanford University, 120 Ocean View Blvd, Pacific Grove, CA 93950, USA. ‡Present Address: 29 Rec Hall, Pennsylvania State University, University Park, PA 16802, USA.

§Author for correspondence (rlcrane@stanford.edu)

R.L.C., 0000-0002-2438-4091; S.M.C., 0000-0002-9704-0716; S.A.K., 0000-0003-3630-2740; S.N.P., 0000-0001-9738-882X

Received 21 December 2017; Accepted 16 April 2018

Journal of Experimental Biology (2018) 221, jeb176099. doi:10.1242/jeb.176099

Mantis shrimp (Crustacea: Stomatopoda) wield lightweight, high-acceleration hammers that strike with small impulses and high peak forces equivalent to a tiger's bite (Huber et al., 2005; Patek and Caldwell, 2005) (Fig. 1A). The hammers move so quickly that water cavitates during impact, such that by wielding their pair of raptorial appendages (second thoracopods), they generate up to four peaks of force (impact and cavitation of both raptorial appendages) (Patek and Caldwell, 2005; Patek et al., 2004). The materials and mechanics of mantis shrimp hammers have been studied extensively (McHenry et al., 2012, 2016; Anderson et al., 2014; Grunenfelder et al., 2014, 2018; Guarín-Zapata et al., 2015; Patek and Caldwell, 2005; Patek et al., 2004, 2007; Suksangpanya et al., 2017; Weaver et al., 2012; Yaraghi et al., 2016). In addition, a physical model of mantis shrimp hammers (Ninjabot) was developed to replicate mantis shrimp strike rotations, accelerations and impacts in water, complete with associated cavitation (Cox et al., 2014) (Fig. 1B). However, mantis shrimp behavioral strategies and the mechanical effectiveness of these strategies have yet to be studied.

Here, we analyzed the behavioral and biomechanical strategies used by mantis shrimp when impacting shells. We measured mantis shrimp feeding behavior and used Ninjabot to compare the effectiveness of feeding strategies. We addressed the following three questions. (1) Do mantis shrimp preferentially strike shells in specific locations? If mantis shrimp strike shells randomly, we would expect strike locations to be distributed evenly across a shell's surface rather than directed at certain regions. (2) Do mantis shrimp target different regions across shell shapes and throughout a strike sequence? If mantis shrimp have behavioral flexibility in how they handle prey, we would expect mantis shrimp to strike shells of different shapes in different locations. Furthermore, the locations that they strike might differ throughout a strike sequence. (3) Do strike locations correspond to shell regions that break most easily? If so, we would expect the strike regions to correspond to the shell regions that are damaged most easily by Ninjabot.

MATERIALS AND METHODS

Animal collection and maintenance

We collected one mantis shrimp species [Crustacea: Stomatopoda: Neogonodactylidae: *Neogonodactylus bredini* (Manning 1969)] and six snail species [*Nerita versicolor* Gmelin 1791, *Nerita peloronta* Linnaeus 1758, *Nerita fulgurans* Gmelin 1791, *Cenchritis muricatus* (Linnaeus 1758), *Cerithium atratum* (Born 1778) and *Cerithium lutosum* Menke 1828] from the Galeta Marine Laboratory, Smithsonian Tropical Research Institute, Panama. Given the similarity of their external morphology, we used *N. versicolor*, *N. peloronta* and *N. fulgurans* interchangeably, and *C. atratum* and *C. lutosum* interchangeably in the experiments described below, resulting in three distinct shell types (Fig. 1C–E). We did not compare or account for differences in internal morphology across these species.

Mantis shrimp and snails were briefly housed locally and then were transported to Duke University, Durham, NC, USA (ANAM Collection Permit no. SE/A-115-13 and SE/A-13-15; Export Permit no. SEX/A-23-14 and SEX/A-17-15). Experiments were performed within 4.5 months of collection. At Duke University, mantis shrimp were housed individually in tanks (20×20×25 cm) in artificial seawater (Instant Ocean Aquarium Sea Salt Mixture, Instant Ocean, Spectrum Brands, Blacksburg, VA, USA) and maintained at 35±1 ppt at 27.4±0.3°C on a 12 h:12 h light:dark cycle. Snails were housed collectively in tanks under the same conditions. Mantis shrimp were fed every 2–3 days with frozen seafood, live grass shrimp and live brine shrimp.

Mantis shrimp feeding behavior

Morphological measurements

We measured mantis shrimp body length (anterior tip of the rostral plate to the posterior tip of the telson) and carapace length (anterior–posterior length of carapace) (0.01 mm resolution; models CD-6″ CX or CD-6″PSX, Mitutoyo Corp., Aurora, IL, USA). Body length and carapace length were tightly correlated (R^2=0.95, t=39.21, n=77 mantis shrimp, P<0.0001). Carapace length was therefore used in analyses as a metric of body size because it was a more consistent metric with lower measurement error standard deviation (s.d.) than body length (mean body length s.d.=0.37 mm; mean carapace length s.d.=0.13 mm). After they molted, mantis shrimp were not used in experiments for at least 10 days to allow for full recovery of striking abilities (Steger and Caldwell, 1983). Molted individuals were then re-measured.

We measured snail shell length (maximum length along the axis of coiling) and then took digital images of the dorsal and ventral

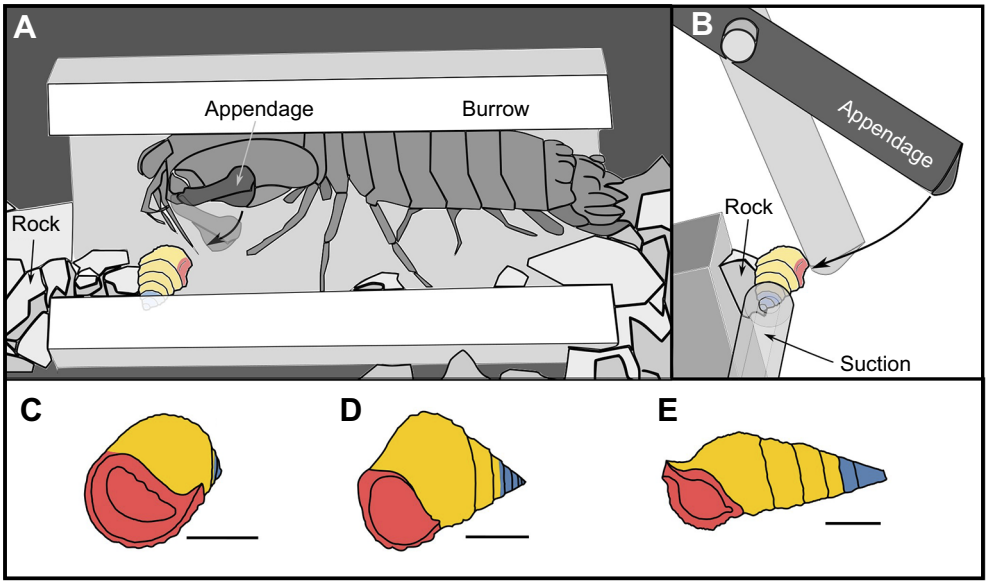

Fig. 1. Smashing mantis shrimp use hammering raptorial appendages to systematically break open a diversity of snail shell shapes. (A) In preparation for a strike, mantis shrimp carefully manipulate the shell into a particular position and then strike it at bullet-like accelerations. (B) We used Ninjabot to perform controlled tests of strike location and shell fracture. Ninjabot is a physical model that strikes with the acceleration and forces of real mantis shrimp (Cox et al., 2014). (C–E) Tests were performed on three shell shapes, shown here divided into the three analyzed shell regions: aperture (red), whorls (yellow) and apex (blue). (C) *Nerita* spp., (D) *Cenchritis muricatus*, (E) *Cerithium* spp. Scale bar: 5 mm.

sides of the snails before and after the experiments (2848×4288 pixel resolution, AF Micro Nikkor 60 mm 1:2.8 D lens with a D300 SLR camera or DX AF-S Nikkor 18-70 mm 1:3.5-4.5G ED lens with a D70 SLR camera, Nikon Corp., Tokyo, Japan). These images were used to quantify shell damage (see 'Snail shell damage measurements', below).

Video collection

We filmed mantis shrimp handling and striking live snails until eating commenced (HDR-PJ790V or HDR-CX900 7.2V, pixel resolution: 1920×1080, frame rate: 30 frames s^{-1}, Sony Corp., Tokyo, Japan). Each mantis shrimp from one group (38 individuals) was fed each of the three snail shapes, and we obtained 87 videos in which the mantis shrimp struck and consumed the snail. The order in which the shells were presented was pseudo-randomly assigned to account for mantis shrimp sex and size. To provide a larger sample size of mantis shrimp handling *Cerithium* spp., which are the focus of the experiments involving the physical model, an additional group of mantis shrimp (39 individuals) was fed only once with *Cerithium* spp. In total, we collected feeding data from 77 mantis shrimp (34 males and 43 females; body length mean±s.d. 38.0±6.1 mm, range 28.5–59.7 mm).

For every feeding experiment, we matched snail shell length with mantis shrimp body size (Fig. S1; *Nerita* spp. length mean±s.d. 10.3±1.6 mm, range 7.5–13.8 mm; *C. muricatus* length mean±s.d. 11.8±2.1 mm, range 8.0–15.5 mm; *Cerithium* spp. length mean±s.d. 13.8±2.5 mm, range 9.3–19.5 mm), based on previous analyses of mantis shrimp snail choice of *Cerithium* spp. in the field (Caldwell et al., 1989). Snail choice is thought to be explained by the energetic balance of the number of strikes and the amount of food obtained relative to snail size (Full et al., 1989). Therefore, we tested for appropriate size matching across snail shapes by comparing the total number of strikes mantis shrimp delivered to each shell shape. We found no significant differences, thus confirming appropriate size matching across snail shapes (Kruskal–Wallis χ^2=1.94, d.f.=2, n=87 strike sequences, P=0.38).

Feeding experiments were performed in glass aquaria with burrows matched to mantis shrimp size (length×diameter: 7×2.5 cm, 6×2 cm, 5×1.3 cm; Steger 1987). Because mantis shrimp often process prey within their burrows, we filmed them in open-sided feeding burrows placed against the side of the tank. Mantis shrimp were acclimated to feeding tanks for a minimum of one night.

Experiments were initiated by dropping a snail, rubbed with freeze-dried krill, into a tank containing a mantis shrimp. If the mantis shrimp did not approach the snail within 5–10 min, the snail was pushed closer to the mantis shrimp. Once the mantis shrimp had touched the snail, nothing was altered in the tank until the end of the video. Filming continued until either the mantis shrimp began eating or 20 min had elapsed since the mantis shrimp had last touched the snail. At the end of each video, the snail was removed. In 48% of the videos, the mantis shrimp struck and ultimately started to eat the snail, and only these videos were used for further analyses.

Video analysis

We coded the location and timing of each strike until the start of feeding (v.7.7.5, Quicktime Pro, Apple Inc., CA, USA). Before they strike, mantis shrimp touch snails with their antennules at the impact location, possibly to measure and align the strike, given that the strike is too fast to adjust after release (Kagaya and Patek, 2016). Because it was not feasible to film these extended strike sequences using high-speed video, we defined impact location as the shell region between the lower tips of the antennules just before a strike. We defined three shell regions: the aperture (including both the inner and outer lip), the whorls (including all the whorls except for the apical-most portion) and the apex (Fig. 1C–E). These definitions accounted for accrued damage such that as a mantis shrimp chipped away at a snail aperture, the newly created lip was considered an aperture strike location. Similarly, as the apex was processed, strikes at the apical-most portion of the snail were coded as the apex. We also recorded the region from which the mantis shrimp started eating.

We accounted for three kinds of error in the video coding: recording a strike that did not occur or failing to record a strike that did occur, incorrect coding of timing of strikes, and incorrect coding of strike location. Two researchers performed the coding and were trained together using the same videos. To assess coding errors, 22 videos were analyzed twice (*Nerita* spp. n=10, *C. muricatus* n=7, *Cerithium* spp. n=5), either by the same researcher or by the two different researchers. The researchers missed a maximum of 2.8% of strikes within each video sequence (most videos had zero missed strikes) and, across all the trials, only 19 strikes out of 1639 total strikes were missed in one of the viewings. Fewer than 1.1% of the strikes were incorrectly coded for timing (incorrect timing defined as differing by more than 0.1 s, corresponding to 3 frames). Approximately 10% of strikes were classified as 'unknown' by one researcher but identified by the other (*Nerita* spp. mean=10.2% of strikes per video, *C. muricatus* mean=10.7%, *Cerithium* spp. mean=8.3%). For strikes where both researchers identified the strike location, instances where they disagreed were distributed as follows: *Nerita* spp. mean=0.7% of strikes per video, *C. muricatus* mean=5.6%, *Cerithium* spp. mean=8.5%.

Physical model experiments

We used a physical model (Ninjabot) that replicates mantis shrimp strike dynamics to test whether mantis shrimp strategically strike *Cerithium* spp. shell regions that break most easily. We struck shells repeatedly in different locations with Ninjabot and quantified the resulting damage (see 'Snail shell damage measurements', below). Ninjabot's mechanism and performance have been reported elsewhere, and closely match the kinematics and strike force of mantis shrimp (Cox et al., 2014). We set Ninjabot's strike force to cause a similar amount of damage after 20 strikes to that produced by a real mantis shrimp after 20 strikes on *Cerithium* spp. We equipped Ninjabot with a stainless steel cylinder appendage with a hydrofoil cross-section (thickness: 5.1 mm; chord length: 9.4 mm) and performed the experiments in water (0 ppt, 21±2°C).

Ninjabot was used to strike *Cerithium* spp. that were suctioned loosely against a rock (n=114 snails, shell length mean±s.d. 20.1±1.2 mm, range 17.0–22.3 mm). Snails were positioned such that they were struck approximately perpendicular to the axis of coiling and normal to the point of contact between the snail and the rock (Fig. 1B). Each snail was struck with the same force 20 times at one of three locations (aperture, n=34 snails; whorls, n=10 snails; or apex, n=35 snails; see 'Video analysis', above, for definitions; Fig. 1C–E) or in a random sequence of these three locations determined by a random number generator (n=35 snails). For every strike, we recorded whether the strike caused any damage and, if so, whether the damage was to the aperture, whorls or apex. To reduce rot, shells had been frozen and were thawed before testing. Snails were photographed before and after the experiment to later quantify shell damage in terms of the amount of shell broken off by Ninjabot (see 'Snail shell damage measurements', below).

Journal of Experimental Biology (2018) 221, jeb176099. doi:10.1242/jeb.176099

Snail shell damage measurements

To quantify shell damage caused by mantis shrimp and Ninjabot, we established new methods to consistently measure damage and then interpret damage in the context of feeding (Fig. 2). We measured apex damage and aperture damage for each shell by comparing photos taken before and after each strike sequence. Mantis shrimp and Ninjabot damaged the aperture by chipping the outer lip such that damage proceeded along a whorl (which wraps around the axis of coiling). Aperture damage was therefore quantified as the number of quarter turns within one complete rotation around the axis of coiling that the damage had reached, generating an ordinal variable (Fig. 2D). For example, snails could be classified as having no damage, having damage between 0 and 1/4 rotations around the axis of coiling, between 1/4 and 1/2 rotations, etc. Because measurement accuracy declined once damage exceeded one full rotation, we categorized damage beyond one rotation as simply greater than one.

Apex damage, in contrast to aperture damage, proceeded along the central axis and was therefore defined as (final apex length−initial apex length)/(initial snail length) (Fig. 2; Fig. S2). Damage that occurred away from the apex or aperture was not measured. Measurement standard deviation was calculated based on three measurements for each snail and was on average 1.0% of the snail length (mean snail length s.d.=0.19 mm) and 10% of the apex length (mean apex length s.d.=0.13 mm).

We used mantis shrimp feeding location data from the behavioral experiments (described in 'Video analysis', above) and shell damage measurements to identify the amount of shell damage necessary for

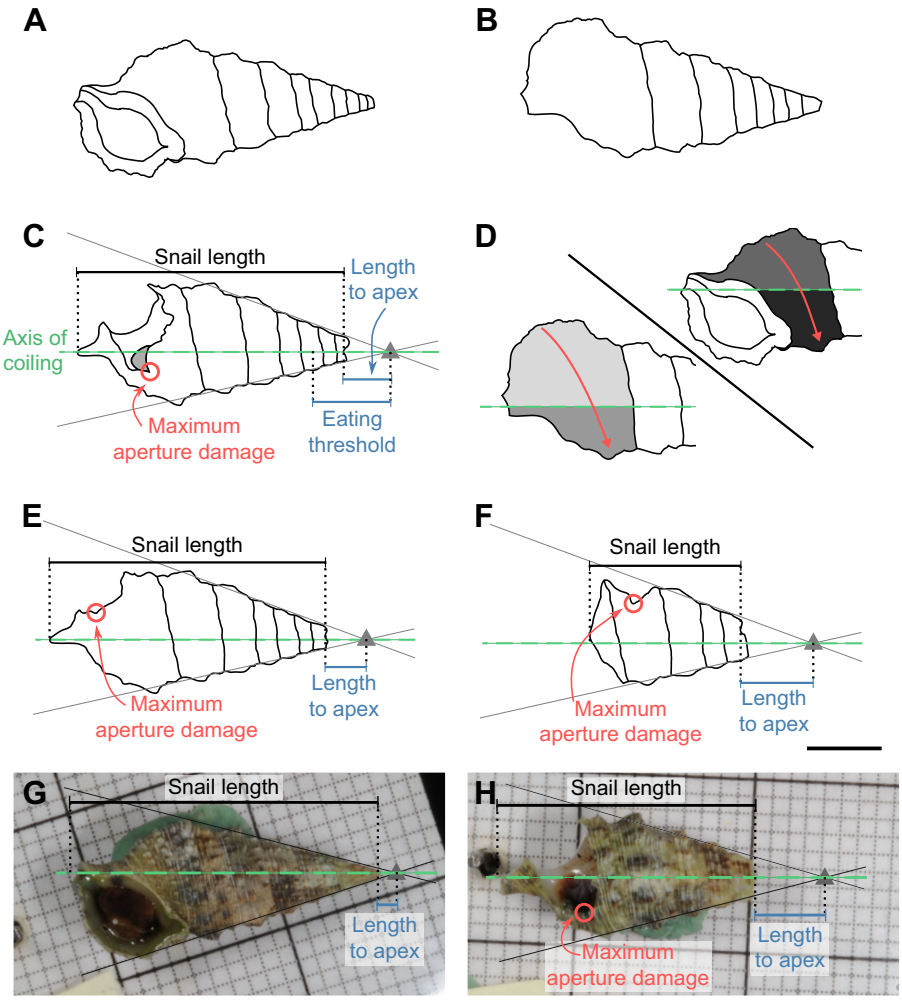

Fig. 2. Snail shell damage measurements. We measured fractured and intact *Cerithium* spp. using measurements that consistently represent shells with varying damage and shape. Traced photographs illustrate a single snail before (A: ventral, B: dorsal) and after (C: dorsal) being struck by Ninjabot, as well as how aperture damage was measured [D: dorsal (left), ventral (right)]. (C) The sloping sides of the shell defined two lines that intersect at a virtual apex point (gray triangle) that persisted in space regardless of whether the snail was damaged or fully intact. Snail length (black line) is the maximum distance between the actual apex and the anterior end of the snail along the central axis of coiling (green dashed line). To calculate the amount of apex broken off, we subtracted the length to apex (blue line) at the end of the experiment from the length to apex at the start of the experiment. The length to apex is the distance between the virtual apex and posterior-most end of the snail, again along the axis of coiling. For aperture damage, we identified the furthest point of damage along the whorl (red circle). In addition, we measured the point at which the mantis shrimp began eating and, with this, established an eating threshold for snails that we used for interpreting the functional importance of the amount of snail breakage. (D) We categorized aperture damage as how many quarter revolutions damage had progressed around the axis of coiling (i.e. along the red arrows). Gray shading indicates the number of quarter revolutions from 1 to 4, with 1 being the lightest and 4 being the darkest (see Materials and Methods). (E,F) The differences between a more intact snail shell (E: dorsal) and more damaged shell (F: dorsal) are thus represented through this suite of measurements, illustrated with digitally manipulated hypothetical quantities of damage to the shell traced in A–D. (G,H) Example measurements of a shell before (G: ventral) and after (H: dorsal) being struck by a mantis shrimp. More example measurements are given in Fig. S2. Scale bar: 5 mm for A–F; G,H photographed on 1 mm square grid.

Journal of Experimental Biology (2018) 221, jeb176099. doi:10.1242/jeb.176099

the mantis shrimp to start eating from the aperture or apex. We used this information to assess whether the Ninjabot experiments caused sufficient damage for the snail to be edible by a mantis shrimp.

Statistical analyses

Do mantis shrimp preferentially strike shells in specific locations?

If mantis shrimp were striking shells randomly, we would expect the proportion of strikes to each region to correspond to the proportion of the shell's surface area within that region. For each shell shape, we measured each region's projected surface area using dorsal and ventral photos (*Nerita* spp. n=3, *C. muricatus* n=4, *Cerithium* spp. n=3 snails), as well as overall surface area of the whole shell. We scaled the null expectation of randomly applied strikes according to each region's proportional surface area. Although projected surface area does not represent three-dimensional shapes, these proportions provide a reasonable null expectation for random striking.

For each shell shape, we tested whether the number of strikes to each region differed from the null expectation of randomly applied strikes (G-test of goodness of fit with repeated measures, totaled across strike sequences; Sokal and Rohlf, 1995) (G-tests conducted in R, RVAide Memoire, Hervé 2017, version 0.9-64). This test is similar to a χ^2 goodness of fit test but allows for repeated measures (i.e. in the case of *Cerithium* spp., there are 62 replicates for the 62 strike sequences in which different mantis shrimp struck their shell repeatedly). The G-test requires taking the natural log, which introduces problems in regions that were never struck. We therefore added one strike to every region in every strike sequence, a conservative change relative to the number of strikes.

Do mantis shrimp target different regions across shell shapes and throughout a strike sequence?

To determine whether mantis shrimp struck different locations depending on shell shape, we compared the proportion of strikes to each region across shell shapes. We conducted paired comparisons and therefore limited our sample to mantis shrimp that successfully completed strike sequences for each of the three shell shapes (n=19 mantis shrimp). We first conducted a paired Friedman's test across the three shell shapes comparing the proportion of strikes to each of the three regions (aperture, whorls or apex). If significant, we ran a *post hoc* paired Wilcoxon signed-rank test with a Bonferroni correction (adjusted α=0.017) examining whether the proportion of strikes to the region differed between each possible pair of shell shapes.

We asked whether mantis shrimp consistently target the same shell regions throughout a strike sequence or whether they instead shift strategies over time. Specifically, we tested whether strikes to certain regions tended to occur earlier or later in a strike sequence. For each shape, we fitted two generalized mixed models: a null model of strike timing with no fixed effect and a full model of strike timing in terms of strike location. All models included individual mantis shrimp strike sequences as random effects. Models were fitted with a log link calculation and a gamma distribution (models fitted in R, lme4, v.1.1.12; Bates et al., 2015). The significance of strike location on strike timing was assessed with a likelihood ratio test between the full and reduced models.

Do strike locations correspond to shell regions that break most easily?

In order to interpret shell damage from the Ninjabot experiments, we used the mantis shrimp feeding experiments to establish eating thresholds, defined as the amount of shell damage required for a mantis shrimp to eat from that region (Fig. 3). The aperture feeding threshold was one-half of a rotation around the central axis: mantis shrimp that fed from the aperture usually surpassed this aperture threshold (6/7 snails), whereas few mantis shrimp that fed from the whorls or apex reached the aperture threshold (3/52 snails). The apex feeding threshold was 20% of the total shell length: almost all mantis shrimp that consumed the shell from the apex passed this threshold (35/36), and no mantis shrimp that ate from the whorls or aperture did (0/8).

Ninjabot shell damage was binned into four categories based on these apex and aperture feeding thresholds: no damage, damage at one-third of the threshold, damage at two-thirds of the threshold,

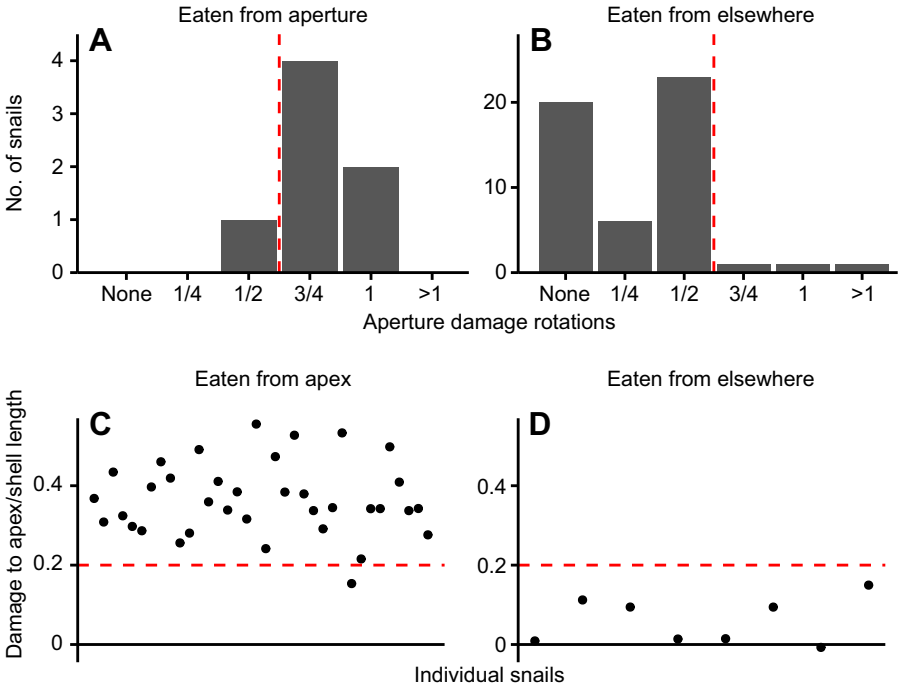

Fig. 3. Determination of eating thresholds. Damage measurements from the behavioral feeding experiments were used to set eating thresholds for the aperture and apex of *Cerithium* spp. (A,B) Aperture damage was categorized as the proportion of a single whorl that was damaged (0, 1/4, 1/2, 3/4, 1) or when the damage exceeded one rotation (>1). For each category of aperture damage, we then counted the number of snails eaten from the aperture (A) or eaten from elsewhere on the snail (B). Note the change in scale of the *y*-axis between A and B. (C,D) Apex damage relative to initial snail length was compared between snails eaten from the apex (C) and snails eaten from elsewhere (D). For both apex and aperture damage datasets, eating thresholds (red dashed lines) were the amount of damage above which the majority of snails could be consumed. These thresholds were used to convert damage from Ninjabot experiments into biologically relevant metrics.

Journal of Experimental Biology (2018) 221, jeb176099. doi:10.1242/jeb.176099

Table 1. Comparing observed with expected strike locations

Snail species	No. of strike sequences	*G*	d.f.	*P*-value	Region	Observed median (IQR)	Observed range	Expected
Nerita spp.	32	3726.6	64	*P*<0.0001	Aperture	0.98 (0.91, 1.00)	0.36–1.00	0.43
					Whorls	0.01 (0.00, 0.07)	0.00–0.64	0.55
					Apex	0.00 (0.00, 0.01)	0.00–0.13	0.02
Cenchritis muricatus	32	6269.5	64	*P*<0.0001	Aperture	0.93 (0.80, 0.99)	0.28–1.00	0.26
					Whorls	0.02 (0.00, 0.06)	0.00–0.33	0.69
					Apex	0.01 (0.00, 0.10)	0.00–0.67	0.05
Cerithium spp.	62	9600.1	124	*P*<0.0001	Aperture	0.30 (0.03, 0.48)	0.00–1.00	0.19
					Whorls	0.01 (0.00, 0.08)	0.00–0.38	0.74
					Apex	0.65 (0.40, 0.92)	0.00–1.00	0.07

A repeated *G*-test of Goodness of Fit assessed, for each shell shape, whether the number of times mantis shrimp struck each region of the shell differed from what would be predicted according to the projected surface area of that shell region. The totaled *G*-test statistic is given, which calculates the effect size for every mantis shrimp strike sequence individually then sums the effects across all mantis shrimp (described further in Materials and Methods). The observed and expected proportions of strikes to each shell region in each strike sequence are reported. IQR, interquartile range.

and damage at or above the threshold. These bins represent the maximum resolution of our ordinal metric of aperture damage. The continuous metric of apex damage was binned by rounding to allow comparisons between aperture and apex damage. Shell damage by Ninjabot that surpassed the threshold indicated instances when mantis shrimp would be able to eat from that region.

We compared the maximum amount of shell damage caused by Ninjabot across the four treatment groups (strikes to the aperture, whorls, apex or random locations) (Kruskal–Wallis test, *post hoc* Wilcoxon rank-sum test with Bonferroni correction, adjusted α=0.0083). Finally, as Ninjabot successively struck the snails, we noted whether damage occurred or not.

All statistical analyses were carried out in R (version 3.3.2, http://www.R-project.org/).

RESULTS

Mantis shrimp struck a mean of 73 times before they started eating (s.d.=72 strikes; median 48 strikes, range 7–460 strikes) with a corresponding mean of 26 min from when the mantis shrimp first touched the shell to when it started eating (s.d.=27 min; median 15 min, range 1.4–133 min). The median time between strikes was 11.3 s. This duration represents how long it takes to set up snails between strikes, but it should be noted that mantis shrimp often performed other behaviors while processing the shell, such as roaming the tank or grooming.

Mantis shrimp positioned and struck shells with a predictable behavioral sequence. First, they rotated the shell using the maxillipeds, sometimes pausing to wiggle the shell into the rocky substrate. Next, they placed their antennules against the shell. The mantis shrimp then either returned to rotating the shell or pulled their antennules out of the way and struck the shell, often causing the shell to be propelled away. They then collected the shell and repeated the sequence. If the shell did not move after being struck, mantis shrimp sometimes skipped setting it up, and simply proceeded to touching it with their antennules and striking.

When analyzing mantis shrimp feeding videos, we excluded all strike sequences in which the strike locations of fewer than half of the strikes could be identified (n=8 strike sequences), and in the remaining videos, if the location of a strike could not be identified, that strike was excluded from analyses of strike location (proportion of unknown strikes in a sequence: mean±s.d. 0.09±0.11, median 0.043).

To enable the statistical tests of mantis shrimp feeding videos described in the subsequent sections, we validated that the proportion of strikes to each region of a shell did not differ significantly between the two groups of mantis shrimp that handled *Cerithium* spp. (mantis shrimp that were fed only *Cerithium* spp. and those fed all three shell shapes). We therefore collapsed the groups for all analyses unless otherwise noted (Wilcoxon rank-sum test, n=62 strike sequences: proportion of strikes to the aperture W=518.5, P=0.31; proportion of strikes to the whorls W=369.5, P=0.23; proportion of strikes to the apex W=403, P=0.51). Here, we define n as the number of individual mantis shrimp strike sequences, as each mantis shrimp only performed one strike sequence while handling *Cerithium* spp.

Similarly, we tested for behavioral differences based on mantis shrimp sex using feedings of *Cerithium* spp., because they constituted our largest sample. The proportion of strikes to each region did not differ significantly between male (n=24 strike sequences) and female (n=38 strike sequences) mantis shrimp, so we collapsed across sex for all further comparisons (Wilcoxon rank-sum test, n=62 strike sequences: proportion of strikes to the aperture W=395.5, P=0.38; proportion of strikes to the whorls W=515, P=0.37; proportion of strikes to the apex W=501, P=0.52).

Do mantis shrimp preferentially strike shells in specific locations?

Mantis shrimp did not strike shells ‘randomly’ (Figs 4 and 5). For each of the shell shapes, the number of strikes to each location differed from the expectation based on proportional projected surface area (Fig. 5A, Table 1). Mantis shrimp struck the whorls less than expected based on surface area. Whether they more frequently struck the apex or aperture depended on shell shape (Fig. 5A, Table 1). Despite strong trends in strike location, individual mantis shrimp varied in terms of where they struck (Fig. 4). Furthermore, individual mantis shrimp often struck shells differently across the three shell shapes and even within single strike sequences (Fig. 4).

Do mantis shrimp target different regions across shell shapes and throughout a strike sequence?

Mantis shrimp struck different regions depending on shell shape. They struck the aperture more when handling low-spired *Nerita* spp. or *C. muricatus* than when handling high-spired *Cerithium* spp. (Table 2, Fig. 5B). They were equally unlikely to strike the whorls regardless of shell shape (Table 2, Fig. 5B). Finally, they struck the apex of high-spired *Cerithium* spp. more frequently than the apex of low-spired *Nerita* spp. or *C. muricatus* (Table 2, Fig. 5B).

Additionally, throughout a feeding bout, mantis shrimp would sometimes shift which regions of a shell they targeted, depending on shell shape. When mantis shrimp handled lower-spired *Nerita* spp. or *C. muricatus*, the timing of strikes to each region did not differ

Journal of Experimental Biology (2018) 221, jeb176099. doi:10.1242/jeb.176099

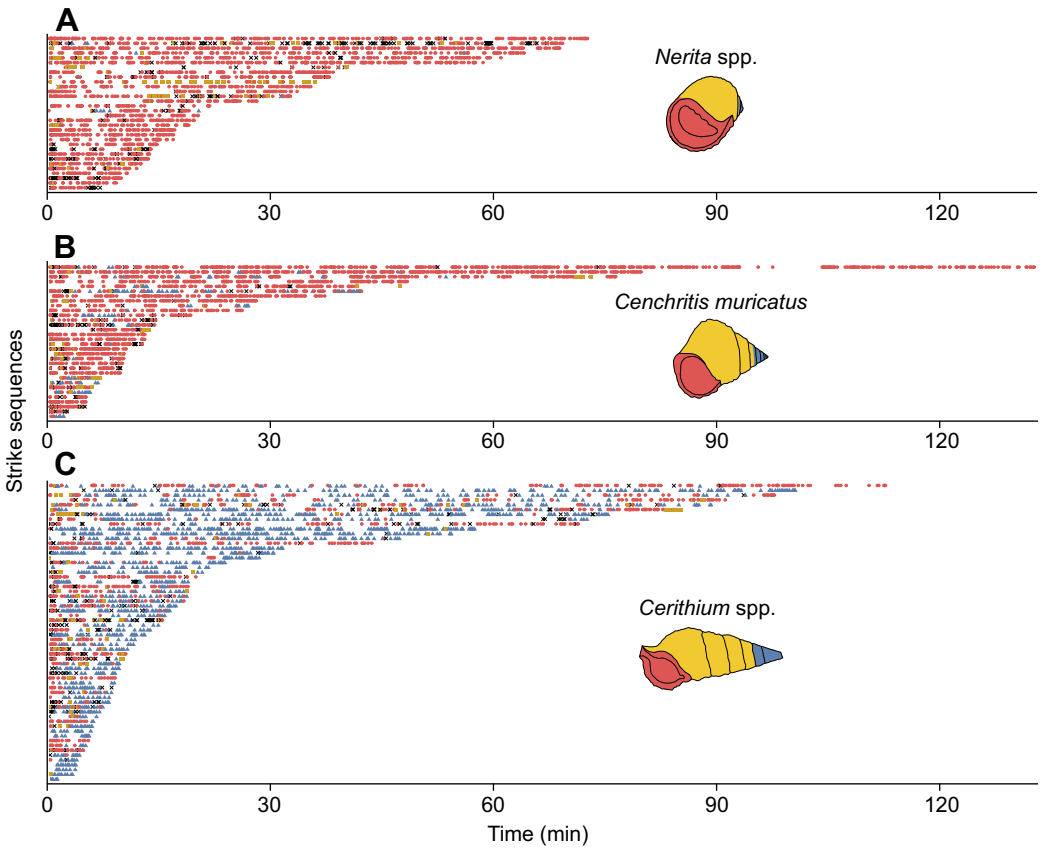

Fig. 4. Strike locations and timing across three shell shapes. Mantis shrimp processed the round shell shapes of (A) *Nerita* spp. and (B) *Cenchritis muricatus* over a wide range of durations while predominantly hitting the aperture (red circles). For the more conical *Cerithium* spp. (C), mantis shrimp predominantly hit the apex (blue triangles), over a similar range of durations. Each row represents an individual mantis shrimp (ordered by feeding duration) and each symbol represents a single strike. Orange squares indicate strikes targeting the whorls and black crosses indicate that the strike location could not be determined from the video. Time zero was set as the first time that the mantis shrimp touched the shell.

(Table 3, Fig. 4), meaning they did not shift strike locations during strike sequences. However, when striking high-spired *Cerithium* spp., mantis shrimp shifted strike locations during strike sequences (Table 3): they struck the apex significantly later in the sequence than the aperture and whorls (Table 3, Fig. 4).

Do strike locations correspond to shell regions that break most easily?

We examined the effectiveness of mantis shrimp strike location strategies against high-spired *Cerithium* spp. by testing whether the locations struck by mantis shrimp correspond to regions of the shell most easily broken by Ninjabot. If strike locations did not differ in their effectiveness, we would expect no difference in the extent of damage across the four Ninjabot treatments (strikes to the aperture, whorls, apex or random locations). Instead, damage to each region differed significantly across the four Ninjabot treatments (Kruskal–Wallis rank-sum test: χ^2=20.4, d.f.=3, P<0.001; Table 4). Ninjabot caused more damage by striking the apex or the aperture than by striking either the whorls or a random sequence of regions (*post hoc* Wilcoxon rank-sum

Table 2. Differences in the proportion of strikes to each shell region between shapes

	Paired Friedman rank-sum test				*Post hoc* paired Wilcoxon signed-rank test		
Shell region	Friedman χ^2	No. of mantis shrimp	d.f.	P-value	Genus comparison	P-value	Bonferroni-adjusted α
Aperture	22.24	19	2	P<0.0001	*Cerithium* & *Cenchritis*	P<0.001	0.017
					Cerithium & *Nerita*	P<0.001	0.017
					Cenchritis & *Nerita*	P=0.30	0.017
Whorls	0.20	19	2	P=0.90	NA	NA	NA
Apex	29.28	19	2	P<0.0001	*Cerithium* & *Cenchritis*	P<0.001	0.017
					Cerithium & *Nerita*	P<0.001	0.017
					Cenchritis & *Nerita*	P=0.16	0.017

The proportion of strikes to the aperture and the proportion of strikes to the apex both differed significantly between shell shapes (paired Friedman rank-sum test), with mantis shrimp striking the aperture less frequently and the apex more frequently when handling *Cerithium* spp. than when handling *Nerita* spp. or *Cenchritis muricatus* (*post hoc* paired Wilcoxon signed-rank test). Mantis shrimp struck the whorls with a similar frequency across all three shell shapes (paired Friedman rank-sum test).

Journal of Experimental Biology (2018) 221, jeb176099. doi:10.1242/jeb.176099

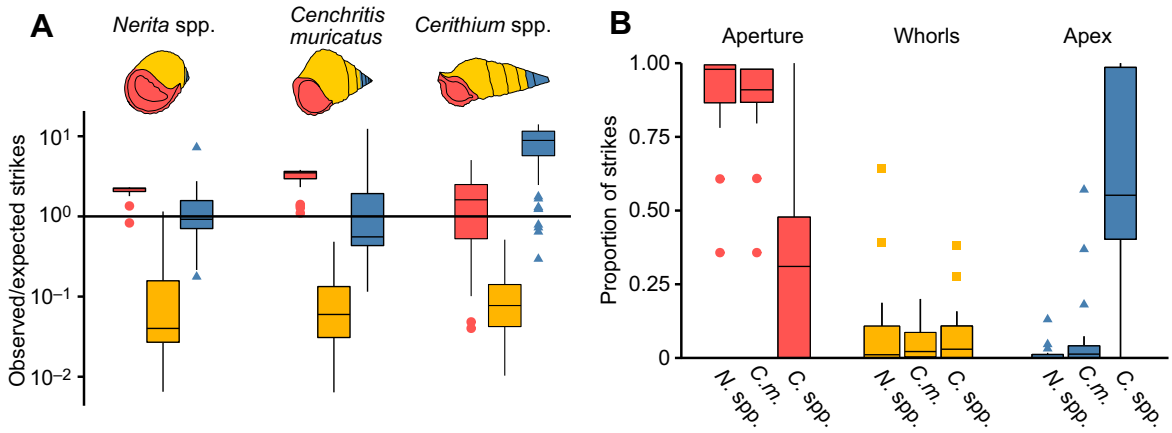

Fig. 5. Mantis shrimp strike snails at different locations depending on the shape of the snail. (A) Low-spired shells (*Nerita* spp., *C. muricatus*) were struck more often on the aperture (red) and less often on the whorls (yellow). 10^0 on the *y*-axis indicates a region that was struck exactly as frequently as would be predicted based on the projected surface area of the snail. The apex (blue) was struck close to expected based on the projected surface area. By contrast, high-spired *Cerithium* spp. were struck disproportionately more on the apex (blue) than on the aperture and whorls. Box plots indicate medians and interquartile ranges (IQRs; whiskers are 1.5× IQR). Sample sizes: *Nerita* spp. and *C. muricatus*: 32 individual mantis shrimp strike sequences; *Cerithium* spp.: 62 individual mantis shrimp strike sequences. Expected proportions of strikes are reported in Table 1. Note, one strike was added to every strike location for every strike sequence to be consistent with the statistical analyses, which required positive values for log-transformed data. (B) The proportion of strikes in a strike sequence was compared across strike locations and shell shapes. To allow for paired comparisons, this graph shows a subset of the data in A: 57 strike sequences from 19 individual mantis shrimp such that each mantis shrimp performed one strike sequence per shell shape. Again, the aperture was struck more often for globular shell shapes and the apex was struck more often for the high-spired shell shape. Whorls were struck equivalently across all shell shapes.

test with Bonferroni-adjusted $\alpha<0.0083$: aperture versus whorls: $P<0.0083$; aperture versus random: $P<0.0083$; apex versus whorls: $P<0.0083$; apex versus random: $P<0.0083$). However, no significant differences emerged between the aperture and apex treatments (*post hoc* Wilcoxon rank-sum test: $P=0.89$) or between the whorls and random treatments ($P=0.25$).

Finally, we used the records of damage associated with each Ninjabot strike to identify the probability of causing damage to the aperture, whorls or apex at any specific strike in a sequence of strikes. The proportion of shells damaged at the aperture was initially high for the first few strikes to the aperture, but this proportion dropped precipitously within the first 10 strikes. The proportion of shells damaged when striking the apex was initially much lower than that for strikes to the aperture, and it fell less steeply. The proportion of shells damaged when striking the whorls remained consistently low (Fig. 6).

DISCUSSION

In spite of their reputation as fierce predators, mantis shrimp typically struck shells many times until they accessed soft tissue. Raptorial appendages are not simple, single-strike weapons, and shells can resist numerous impacts (Fig. 4). Mantis shrimp preceded raptorial strikes with a series of behaviors including touching, probing and positioning the shell. This process of setting up the shell took a median of 11.3 s per strike, far longer than the millisecond duration of the strike itself. Orienting and stabilizing the shell presented challenges to the mantis shrimp; shells would frequently wobble or fall over as soon as a mantis shrimp released them. After a strike, the snail was often propelled away from the original site, reinitiating the entire set-up process.

Depending on shell shape, mantis shrimp struck different shell regions and, for certain shell shapes, changed strike locations within a strike sequence. They most often struck the aperture of globular shells (*Nerita* spp.) and medium-spired shells (*C. muricatus*). In contrast, they targeted the aperture and apex of high-spired shells (*Cerithium* spp.), but with large variation in strategy between individuals and within strike sequences. When striking high-spired shells, mantis shrimp tended to shift strike location from the aperture to the apex, unlike the constant location strategies used for processing lower-spired shells. For all shell shapes, they avoided the whorls, striking them with a median of only 1/100th the expected frequency based on projected surface area. Even though the whorls dominate shell surface area and correspond to the location of soft tissue, mantis shrimp focused on peripheral regions characterized by fine features and edges.

Why would mantis shrimp strike the aperture of lower-spired shells persistently throughout a strike sequence, but change strike locations from aperture to apex of high-spired shells? Starting with the aperture is unlikely to make it easier to break the apex: fractures tend to propagate along, or parallel to, the sutures between whorls as

Table 3. Mantis shrimp shift strike locations throughout a strike sequence only when striking high-spired *Cerithium* spp.

Snail species	No. of strikes	No. of strike sequences	χ^2	*P*-value	Full AIC	Reduced AIC	Coefficient	Estimate
Nerita spp.	2826	32	4.1	$P=0.13$	21878	21878	–	–
Cenchritis muricatus	2724	32	4.9	$P=0.08$	20772	20773	–	–
Cerithium spp.	2953	62	64.3	$P<0.0001$	22732	22792	Intercept	2.18
							Aperture	–0.31
							Whorls	–0.44

When striking *Nerita* spp. or *Cenchritis muricatus*, mantis shrimp did not shift strike locations. The sequences of strike regions and timing were assessed separately for each shell shape. Two generalized mixed models were used, one with and one without strike region applied as a fixed effect. Individual strike sequence was included as a random effect, and the two models were compared via a likelihood ratio test. AIC, Akaike's information criterion.

Journal of Experimental Biology (2018) 221, jeb176099. doi:10.1242/jeb.176099

Table 4. Ninjabot causes the most damage when striking the aperture or apex

Shell region struck	Shell region measured	No damage	1/3 damage	2/3 damage	Able to be eaten
Aperture	Aperture	**8**	**5**	**20**	**1**
	Apex	31	2	1	0
Whorls	Aperture	9	1	0	0
	Apex	7	2	1	0
Apex	Aperture	28	7	0	0
	Apex	**4**	**14**	**12**	**5**
Random	Aperture	20	11	4	0
	Apex	21	13	1	0

The damage resulting from strikes to specific shell regions was categorized as no damage, 1/3 damage, 2/3 damage or able to be eaten. Each shell was tested once and the number of shells in each damage category is indicated. Bold values indicate instances where the strike location corresponds to the region where damage was measured.

opposed to crossing them, such that for a high-spired shell, cracks are unlikely to propagate all the way to the apex (Blundon and Vermeij, 1983). Instead, we propose that mantis shrimp first target the easiest region to damage (the thin edges of the aperture) and then switch to another region if that first approach fails. Other predators, including other crustaceans, show similar behavioral flexibility in attack strategy (Edgell and Rochette, 2009; Schaefer and Zimmer, 2013; Zipser and Vermeij, 1978), and mantis shrimp possess neuroanatomical features associated with such levels of memory and complex behaviors (Wolff et al., 2017).

Consistent with mantis shrimp behavior, when striking high-spired *Cerithium* spp., Ninjabot more effectively fractured the aperture and apex than the whorls or a random sequence of strike locations. Ninjabot caused little damage when striking the whorls, and mantis shrimp also avoided this effectively armored region. However, measurements of total shell damage showed Ninjabot was equally effective at damaging the aperture and apex, which suggests that the mantis shrimp's strategy of striking the aperture first does not reflect that, across a strike sequence, the aperture or apex is easier to fracture.

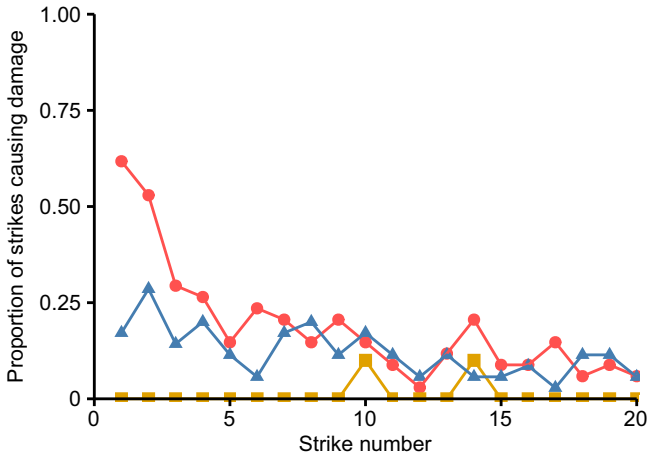

Fig. 6. Effectiveness of strike locations. Shell damage across a series of strikes performed by Ninjabot against *Cerithium* spp. initially occurred at a higher rate for shells struck at the aperture (red circles, n=34 shells) than for those struck at the apex (blue triangles, n=35 shells) or whorls (yellow squares, n=10 shells), and then rapidly converged to a low amount of damage across the three treatment groups.

Damage patterns within strike sequences offer insight into why mantis shrimp shift strike locations when handling high-spired *Cerithium* spp. Ninjabot showed that the probability of causing damage to the aperture, although initially particularly high, drops off steeply as the number of strikes increases (Fig. 6). This finding that the aperture of high-spired *Cerithium* spp. is easy to damage, but further damage is increasingly difficult, corresponds to mantis shrimp behavioral patterns when handling high-spired shells. Furthermore, eating thresholds and patterns of shell damage present additional evidence that further fracturing a shell becomes more difficult as the shell is damaged, especially at the aperture. Few shells struck by Ninjabot on either the aperture or apex were damaged beyond the threshold for a mantis shrimp to start eating, but many shells were damaged to two-thirds of that threshold (Table 4). Similarly, in the mantis shrimp feeding experiments, the shell region from which the snail was not consumed (i.e. the aperture of a shell for snails consumed from the apex, and vice versa) often sustained moderate damage just shy of the eating threshold (Fig. 3). The prevalence of shells in both experiments that almost reached the threshold suggests that damaging a shell increases in difficulty. The many shells from the behavioral experiments that sustained damage to two-thirds of the aperture eating threshold, but were ultimately consumed at the apex, highlights the biological relevance for mantis shrimp behavior of diminishing returns in shell damage at the aperture (Fig. 3).

Shell morphology may illuminate why strikes to the aperture become less effective as the shell is damaged. Non-fatal damage to the aperture in the behavioral experiments often wrapped just over half-way around the first whorl (Fig. 3), corresponding to the location of the most anterior varix – a repeating, regularly spaced thickened ridge running across a whorl parallel to the central axis. Because varices defend against aperture-pealing predators (Savazzi, 1991; Zuschin et al., 2003), the anterior-most varix could set a threshold of diminishing returns for aperture strikes. In the context of shell evolution, thickening the entire shell would be costly and unnecessary if a thickened varix were sufficient to arrest damage and the snail could withdraw past this point. High-spired snails are able to withdraw further into their shells (Edgell and Miyashita, 2009), which matches our observations of *Cerithium* spp. (R.L.C., unpublished observations), the only shell shape used in the behavioral experiments that possesses varices.

In addition to shell fracture resistance, other aspects of mantis shrimp attacks potentially also affect mantis shrimp strategy. Stably setting up shells for ballistic strikes may influence strike location. For example, for globular shells, the most stable orientation may present only the aperture to the mantis shrimp, whereas the most stable orientations for higher-spired shells could present multiple regions. Similarly, morphological cues, like sharp edges or small peripheral features, may be more ambiguous on high-spired shells than on globular shells, resulting in more variation in strike location. Further research on how mantis shrimp set up shells and identify potential strike locations may elucidate nuances of the strike location strategy. Although future studies would benefit from high-speed imaging to more accurately identify strike locations, at present, high-speed cameras do not have sufficient buffering capacity to store long strike sequences.

Broader implications and conclusions

Jaw- and claw-based predators that slowly apply forces both share features with and are distinct from predators using transient, high-force impacts. Animals that slowly load shells use real-time feedback to the nervous system, allowing them to adjust their

behavior and force application as they process prey. In contrast, mantis shrimp strikes are feed-forward movements that require advanced planning: the strike is so brief that it is not possible to shift strategy once the strike begins (Kagaya and Patek, 2016; Patek, 2015). Mantis shrimp's extensive pre-strike behaviors may reflect that they must acquire visual and tactile sensory information prior to striking.

Behavioral flexibility, with a focus on the aperture and apex, unites mantis shrimp and many crushing-based predators. Crabs with strong claws relative to prey size often crush the shell, create a hole in the body whorl or cut the shell in half (Edgell and Rochette, 2009; Elner, 1978; Behrens Yamada and Boulding, 1998; Zipser and Vermeij, 1978). With more challenging prey, crabs often focus distally, severing the spire of high-spired shells or peeling the aperture, if it is sufficiently large (Edgell and Rochette, 2009; Behrens Yamada and Boulding, 1998; Zipser and Vermeij, 1978). Like crabs handling large snails, mantis shrimp in size-matched experiments focused on the aperture and apex. Furthermore, crabs apply repeated crushing loads and attempt different crushing orientations, and when peeling the aperture, they pry the shell in a manner that differs from their crushing attacks (Boulding and LaBarbera, 1986; Elner, 1978; Zipser and Vermeij, 1978). In contrast, mantis shrimp used tens to hundreds of strikes, relying on the same striking motion to consistently chip at the shell.

A benefit of high-acceleration hammers may be access to large snails relative to the predator's body size, given that the shells need not fit within the gape of a claw or mouth. Nonetheless, the energetic costs of repeated strikes and extensive behavioral set-ups may limit the benefits of impact fracture. Mantis shrimp work for days to crack open a large shell in the laboratory (S.N.P., unpublished observation), yet they prefer moderately sized shells when given the choice (Full et al., 1989). In the wild, where mantis shrimp have their own predators to avoid, working on cracking open a shell for hours or days may not be a viable option. Whether mantis shrimp, like crabs, use different behavioral strategies depending on the relative size of their prey remains an unanswered and promising area of further research.

Interpretation of shell fracture is significant for both extant and extinct systems and is a major component of ecological and evolutionary studies (Kowalewski et al., 1998; Oji et al., 2003; Vermeij, 1977; Zuschin et al., 2003). Shell damage and predator weapon evolution in the fossil record illuminate the arms race between hard-shelled prey and their predators (Bicknell and Paterson, 2017; Haug et al., 2010; Kowalewski et al., 1998; Vermeij, 1977). Just as the mantis shrimp weapon is in fact a generalist weapon, capable of being used effectively in a variety of contexts (deVries et al., 2016; deVries, 2017; Green and Patek, 2015, 2018), snail shells must also defend against a variety of threats. Shell fracture analyses across different predatory strategies promise to further explain this many-partied evolutionary escalation between shelled prey and their predators.

This study lays the groundwork for future studies of impact fracture in biology, provides a functional context for studies of mantis shrimp hammer material design (Grunenfelder et al., 2014, 2018; Guarín-Zapata et al., 2015; Suksangpanya et al., 2017; Weaver et al., 2012; Yaraghi et al., 2016) and models an approach for integrating animal behavior and physical modeling to elucidate complicated physical processes. Ninjabot enabled controlled testing and interpretation of mantis shrimp behavioral strategies, including those outside the mantis shrimp's repertoire, and thus yielded insight into underlying fracture mechanics. Our simplified coding system for complex shell architectures can be applied to different shell shapes and facilitates studies of comparable strike locations across diverse shell shapes and behavioral strategies. Impact fracture is a rich field offering insights into animal behavior, biomaterials and the evolutionary escalation of predators and prey.

Acknowledgements
We are grateful to John Christy and the Galeta Marine Lab staff, Smithsonian Tropical Research Institute, for facilitating our work in Panama. We thank Patrick Green and Maya deVries for help with animal collection, Wilson Brace, Leah Fitchett and Erin Choe for data collection assistance, and Patek Lab members and two anonymous reviewers for comments and feedback on the manuscript.

Competing interests
The authors declare no competing or financial interests.

Author contributions
Conceptualization: R.L.C., S.M.C., S.N.P.; Methodology: R.L.C., S.M.C., S.A.K., S.N.P.; Software: R.L.C., S.M.C.; Validation: R.L.C., S.A.K.; Formal analysis: R.L.C., S.M.C.; Investigation: R.L.C., S.M.C., S.A.K.; Data curation: R.L.C., S.M.C.; Writing - original draft: R.L.C., S.M.C., S.N.P.; Writing - review & editing: R.L.C., S.M.C., S.A.K., S.N.P.; Visualization: R.L.C., S.M.C.; Supervision: S.N.P.; Project administration: R.L.C.

Funding
This research was funded by a National Science Foundation grant (IOS 1439850) to S.N.P.

Data availability
Data are available from the Dryad Digital Repository (Crane et al., 2018): https://doi.org/10.5061/dryad.5mp83f1.

Supplementary information
Supplementary information available online at
http://jeb.biologists.org/lookup/doi/10.1242/jeb.176099.supplemental

References
Anderson, P. S. L., Claverie, T. and Patek, S. N. (2014). Levers and linkages: mechanical trade-offs in a power-amplified system. *Evolution* **68**, 1919-1933.
Baldridge, A. K. and Smith, L. D. (2008). Temperature constraints on phenotypic plasticity explain biogeographic patterns in predator trophic morphology. *Mar. Ecol. Prog. Ser.* **365**, 25-34.
Bates, D., Mächler, M., Bolker, B. M. and Walker, S. C. (2015). Fitting linear mixed-effects models using lme4. *J. Stat. Softw.* **67**, 1-48.
Behrens Yamada, S. and Boulding, E. G. (1998). Claw morphology, prey size selection and foraging efficiency in generalist and specialist shell-breaking crabs. *J. Exp. Mar. Bio. Ecol.* **220**, 191-211.
Bicknell, R. D. C. and Paterson, J. R. (2017). Reappraising the early evidence of durophagy and drilling predation in the fossil record: implications for escalation and the Cambrian Explosion. *Biol. Rev. Camb. Philos. Soc.* **93**, 754-784
Blundon, J. A. and Vermeij, G. J. (1983). Effect of shell repair on shell strength in the gastropod *Littorina irrorata*. *Mar. Biol.* **76**, 41-45.
Boulding, E. G. and LaBarbera, M. (1986). Fatigue damage: repeated loading enables crabs to open larger bivalves. *Biol. Bull.* **171**, 538-547.
Bourdeau, P. E. (2010). An inducible morphological defence is a passive by-product of behaviour in a marine snail. *Proc. R. Soc. B Biol. Sci.* **277**, 455-462.
Buschbaum, C., Buschbaum, G., Schrey, I. and Thieltges, D. W. (2007). Shell-boring polychaetes affect gastropod shell strength and crab predation. *Mar. Ecol. Prog. Ser.* **329**, 123-130.
Caldwell, R. L., Roderick, G. K. and Shuster, S. M. (1989). Studies of predation by *Gonodactylus bredini*. In *Biology of Stomatopods*, Vol. 3 (ed. E.A. Ferrero), pp. 117-131. Modena: Mucchi.
Chai, H., Lee, J. J.-W., Constantino, P. J., Lucas, P. W. and Lawn, B. R. (2009). Remarkable resilience of teeth. *Proc. Natl. Acad. Sci. USA* **106**, 7289-7293.
Constantino, P. J., Lee, J. J.-W., Morris, D., Lucas, P. W., Hartstone-Rose, A., Lee, W.-K., Dominy, N. J., Cunningham, A., Wagner, M. and Lawn, B. R. (2011). Adaptation to hard-object feeding in sea otters and hominins. *J. Hum. Evol.* **61**, 89-96.
Cox, S. M., Schmidt, D., Modarres-Sadeghi, Y. and Patek, S. N. (2014). A physical model of the extreme mantis shrimp strike: kinematics and cavitation of Ninjabot. *Bioinspir. Biomim.* **16014**, 1-16.
Crane, R. L., Cox, S. M., Kisare, S. A. and Patek, S. N. (2018). Data from: Smashing mantis shrimp strategically impact shells. Dryad Digital Repository. https://doi.org/10.5061/dryad.5mp83f1
Crofts, S. B. and Summers, A. P. (2014). How to best smash a snail: the effect of tooth shape on crushing load. *J. R. Soc. Interface* **11**, 20131053.

deVries, M. S. (2017). The role of feeding morphology and competition in governing the diet breadth of sympatric stomatopod crustaceans. *Biol. Lett.* **13**, 2017055.
deVries, M. S., Murphy, E. A. K. and Patek, S. N. (2012). Strike mechanics of an ambush predator: the spearing mantis shrimp. *J. Exp. Biol.* **215**, 4374-4384.
deVries, M. S., Stock, B. C., Christy, J. H., Goldsmith, G. R. and Dawson, T. E. (2016). Specialized morphology corresponds to a generalist diet: linking form and function in smashing mantis shrimp crustaceans. *Oecologia* **182**, 429-442.
Edgell, T. C. and Miyashita, T. (2009). Shell shape and tissue withdrawal depth in 14 species of temperate intertidal snail. *J. Molluscan Stud.* **75**, 235-240.
Edgell, T. C. and Rochette, R. (2008). Differential snail predation by an exotic crab and the geography of shell-claw covariance in the northwest Atlantic. *Evolution.* **62**, 1216-1228.
Edgell, T. C. and Rochette, R. (2009). Prey-induced changes to a predator's behaviour and morphology: implications for shell-claw covariance in the northwest Atlantic. *J. Exp. Mar. Bio. Ecol.* **382**, 1-7.
Elner, R. W. (1978). The mechanics of predation by the shore crab, *Carcinus maenas* (L.), on the edible mussel, *Mytilus edulis* L. *Oecologia* **36**, 333-344.
Fisher, J. A. D. (2010). Parasite-like associations in rocky intertidal assemblages: implications for escalated gastropod defenses. *Mar. Ecol. Prog. Ser.* **399**, 199-209.
Full, R. J., Caldwell, R. L. and Chow, S. W. (1989). Smashing energetics: prey selection and feeding efficiency of the stomatopod, *Gonodactylus bredini*. *Ethology* **81**, 134-147.
Green, P. A. and Patek, S. N. (2015). Contests with deadly weapons: telson sparring in mantis shrimp (Stomatopoda). *Biol. Lett.* **11**, 20150558.
Green, P. A. and Patek, S. N. (2018). Mutual assessment during ritualized fighting in mantis shrimp (Stomatopoda). *Proc. R. Soc. B Biol. Sci.* **285**, 20172542.
Grunenfelder, L. K., Suksangpanya, N., Salinas, C., Milliron, G., Yaraghi, N., Herrera, S., Evans-Lutterodt, K., Nutt, S. R., Zavattieri, P. and Kisailus, D. (2014). Bio-inspired impact-resistant composites. *Acta Biomater.* **10**, 3997-4008.
Grunenfelder, L. K., Milliron, G., Herrera, S., Gallana, I., Yaraghi, N., Hughes, N., Evans-Lutterodt, K., Zavattieri, P. and Kisailus, D. (2018). Ecologically driven ultrastructural and hydrodynamic designs in Stomatopod cuticles. *Adv. Mater.* **30**, 1705295.
Guarín-Zapata, N., Gomez, J., Yaraghi, N., Kisailus, D. and Zavattieri, P. D. (2015). Shear wave filtering in naturally-occurring Bouligand structures. *Acta Biomater.* **23**, 11-20.
Haug, J. T., Haug, C., Maas, A., Kutschera, V. and Waloszek, D. (2010). Evolution of mantis shrimps (Stomatopoda, Malacostraca) in the light of new Mesozoic fossils. *BMC Evol. Biol.* **10**, 1-17.
Huber, D. R., Eason, T. G., Hueter, R. E. and Motta, P. J. (2005). Analysis of the bite force and mechanical design of the feeding mechanism of the durophagous horn shark *Heterodontus francisci*. *J. Exp. Biol.* **208**, 3553-3571.
Kagaya, K. and Patek, S. N. (2016). Feed-forward motor control of ultrafast, ballistic movements. *J. Exp. Biol.* **219**, 319-333.
Kolmann, M. A., Crofts, S. B., Dean, M. N., Summers, A. P. and Lovejoy, N. R. (2015). Morphology does not predict performance: jaw curvature and prey crushing in durophagous stingrays. *J. Exp. Biol.* **218**, 3941-3949.
Kowalewski, M., Dulai, A. and Fürsich, F. T. (1998). A fossil record full of holes: the Phanerozoic history of drilling predation. *Geology* **26**, 1091-1094.
Le Rossignol, A. P., Buckingham, S. G., Lea, S. E. G. and Nagarajan, R. (2011). Breaking down the mussel (*Mytilus edulis*) shell: which layers affect Oystercatchers' (*Haematopus ostralegus*) prey selection? *J. Exp. Mar. Bio. Ecol.* **405**, 87-92.
Lucas, P., Constantino, P., Wood, B. and Lawn, B. (2008). Dental enamel as a dietary indicator in mammals. *BioEssays* **30**, 374-385.
McHenry, M. J., Claverie, T., Rosario, M. V. and Patek, S. N. (2012). Gearing for speed slows the predatory strike of a mantis shrimp. *J. Exp. Biol.* **215**, 1231-1245.
McHenry, M. J., Anderson, P. S. L., Van Wassenbergh, S., Matthews, D. G., Summers, A. P. and Patek, S. N. (2016). The comparative hydrodynamics of rapid rotation by predatory appendages. *J. Exp. Biol.* **219**, 3399-3411.
Nagarajan, R., Lea, S. E. G. and Goss-Custard, J. D. (2002). Mussel valve discrimination and strategies used in valve discrimination by the oystercatcher, *Haematopus ostralegus*. *Funct. Ecol.* **16**, 339-345.
Nagarajan, R., Lea, S. E. G. and Goss-Custard, J. D. (2015). Do oystercatchers (*Haematopus ostralegus*) select the most profitable limpets (*Patella* spp.)? *J. Exp. Mar. Bio. Ecol.* **464**, 26-34.
Oji, T., Ogaya, C. and Takehiro, S. (2003). Increase of shell-crushing predation recorded in fossil shell fragmentation. *Paleobiology* **29**, 520-526.
Patek, S. N. (2015). The most powerful movements in biology: from jellyfish stingers to mantis shrimp appendages, it takes more than muscle to move extremely fast. *Am. Sci.* **103**, 330-338.
Patek, S. N. and Caldwell, R. L. (2005). Extreme impact and cavitation forces of a biological hammer: strike forces of the peacock mantis shrimp *Odontodactylus scyllarus*. *J. Exp. Biol.* **208**, 3655-3664.
Patek, S. N., Korff, W. L. and Caldwell, R. L. (2004). Deadly strike mechanism of a mantis shrimp. *Nature* **428**, 819-820.
Patek, S. N., Nowroozi, B. N., Baio, J. E., Caldwell, R. L. and Summers, A. P. (2007). Linkage mechanics and power amplification of the mantis shrimp's strike. *J. Exp. Biol.* **210**, 3677-3688.
Preston, S. J., Revie, I. C., Orr, J. F. and Roberts, D. (1996). A comparison of the strengths of gastropod shells with forces generated by potential crab predators. *J. Zool.* **238**, 181-193.
Savazzi, E. (1991). Constructional morphology of strombid gastropods. *Lethaia* **24**, 311-331.
Schaefer, G. and Zimmer, M. (2013). Ability of invasive green crabs to handle prey in a recently colonized region. *Mar. Ecol. Prog. Ser.* **483**, 221-229.
Smith, L. D. and Palmer, A. R. (1994). Effects of manipulated diet on size and performance of brachyuran crab claws. *Science* **264**, 710-712.
Sokal, R. R. and Rohlf, F. J. (1995). *Biometry: The Principles and Practice of Statistics in Biological Research*, 3rd edition. New York: W.H. Freeman and Company.
Steger, R. (1987). Effects of refuges and recruitment on gonodactylid stomatopods, a guild of mobile prey. *Ecology* **68**, 1520-1533.
Steger, R. and Caldwell, R. L. (1983). Intraspecific deception by bluffing: a defense strategy of newly molted stomatopods (arthropoda: crustacea). *Science* **221**, 558-560.
Suksangpanya, N., Yaraghi, N. A., Kisailus, D. and Zavattieri, P. (2017). Twisting cracks in Bouligand structures. *J. Mech. Behav. Biomed. Mater.* **76**, 38-57.
Taylor, D. (2016). Impact damage and repair in shells of the limpet *Patella vulgata*. *J. Exp. Biol.* **219**, 3927-3935.
Vermeij, G. J. (1977). The mesozoic marine revolution: evidence from snails, predators and grazers. *Paleobiology* **3**, 245-258.
Vermeij, G. J. (1987). *Evolution and Esclation: An Ecological History of Life*. Princeton, NJ: Princeton University Press.
Vermeij, G. J. and Currey, J. D. (1980). Geographical variation in the strength of thaidid snail shells. *Biol. Bull.* **158**, 383-389.
Weaver, J. C., Milliron, G. W., Miserez, A., Evans-Lutterodt, K., Herrera, S., Gallana, I., Mershon, W. J., Swanson, B., Zavattieri, P., DiMasi, E. et al. (2012). The stomatopod dactyl club: a formidable damage-tolerant biological hammer. *Science* **336**, 1275-1280.
West, K., Cohen, A. and Baron, M. (1991). Morphology and behavior of crabs and gastropods from Lake Tanganyika, Africa: implications for lacustrine predator-prey coevolution. *Evolution* **45**, 589-607.
Wolff, G. H., Thoen, H. H., Marshall, J., Sayre, M. E. and Strausfeld, N. J. (2017). An insect-like mushroom body in a crustacean brain. *Elife* **6**, e29889.
Yaraghi, N. A., Guarín-Zapata, N., Grunenfelder, L. K., Hintsala, E., Bhowmick, S., Hiller, J. M., Betts, M., Principe, E. L., Jung, J.-Y., Sheppard, L. et al. (2016). A sinusoidally architected helicoidal biocomposite. *Adv. Biomater.* **28**, 6835-6844.
Zipser, E. and Vermeij, G. J. (1978). Crushing behavior of tropical and temperate crabs. *J. Exp. Mar. Bio. Ecol.* **31**, 155-172.
Zuschin, M., Stachowitsch, M. and Stanton, R. J. J. (2003). Patterns and processes of shell fragmentation in modern and ancient marine environments. *Earth-Science Rev.* **63**, 33-82.